SpyLigase peptide–peptide ligation polymerizes affibodies to enhance magnetic cancer cell capture

Jacob O. Fierer[1], Gianluca Veggiani[1], and Mark Howarth[2]

Department of Biochemistry, University of Oxford, Oxford, OX1 3QU, United Kingdom

Edited by David A. Tirrell, California Institute of Technology, Pasadena, CA, and approved February 25, 2014 (received for review August 22, 2013)

Individual proteins can now often be modified with atomic precision, but there are still major obstacles to connecting proteins into larger assemblies. To direct protein assembly, ideally, peptide tags would be used, providing the minimal perturbation to protein function. However, binding to peptides is generally weak, so assemblies are unstable over time and disassemble with force or harsh conditions. We have recently developed an irreversible protein–peptide interaction (SpyTag/SpyCatcher), based on a protein domain from *Streptococcus pyogenes*, that locks itself together via spontaneous isopeptide bond formation. Here we develop irreversible peptide–peptide interaction, through redesign of this domain and genetic dissection into three parts: a protein domain termed SpyLigase, which now ligates two peptide tags to each other. All components expressed efficiently in *Escherichia coli* and peptide tags were reactive at the N terminus, at the C terminus, or at internal sites. Peptide–peptide ligation enabled covalent and site-specific polymerization of affibodies or antibodies against the tumor markers epidermal growth factor receptor (EGFR) and HER2. Magnetic capture of circulating tumor cells (CTCs) is one of the most promising approaches to improve cancer prognosis and management, but CTC capture is limited by inefficient recovery of cells expressing low levels of tumor antigen. SpyLigase-assembled protein polymers made possible the isolation of cancerous cells expressing lower levels of tumor antigen and should have general application in enhancing molecular capture.

bionanotechnology | synthetic biology | metastasis | antibody | nanobiotechnology

Peptide tags are powerful tools for analyzing protein function, but have major limitations for controlling protein function (1, 2). The flexibility and small surface area of peptides mean that peptide interactions are typically weak and reversible (3), and generally depend on binding of large protein partners (4–6). These restrictions limit how peptides can be used for nanoassembly and synthetic biology (7–9). We sought to develop irreversible covalent interaction between two peptides; we desired all parts to be genetically encoded, with no cysteines involved, and with flexibility in location of the peptide tags. Covalent reaction would enable peptide interactions to resist force, as the strongest noncovalent interactions can be broken by molecular motors (10) or by the forces acting during cell isolation (11).

CnaB2 is a domain from the fibronectin adhesion protein FbaB of *Streptococcus pyogenes* (Spy), essential for the bacteria to invade human cells (12). Within CnaB2, there is a spontaneous reaction to form an isopeptide bond between Lys and Asp, catalyzed by an apposed Glu (Fig. 1*A*) (13, 14). We previously showed that the CnaB2 domain could be split into two parts to enable protein–peptide ligation, via isopeptide bond formation between a peptide tag (i.e., SpyTag) and a protein domain (i.e., SpyCatcher) (15). Here we establish how CnaB2 can be split into three parts to enable peptide–peptide ligation.

We applied peptide–peptide ligation to address a major challenge in cell isolation. Isolation of rare cells has applications in stem cell therapy (16), adoptive immunotherapy (17), and the capture of circulating tumor cells (CTCs). Analyzing CTCs is one of the most promising ways to improve cancer prognosis and to personalize therapy according to the expression pattern of each individual's cancer (18). CTC isolation is a great challenge because of the low frequency of CTCs (one CTC in 10^6–10^9 normal leukocytes) and the heterogeneous antigen expression of CTCs (18). The difficulty of capturing CTCs expressing low levels of tumor marker is an important limiting factor, leading to a high frequency of false-negative results in CTC testing (18, 19). We previously showed that isolation of low-expressing cells depends on ultrastable interactions between the binding protein and the magnetic bead, as well as formation of a large number of contacts at the bead:cell synapse (11). Magnetic cell capture is typically performed with beads bearing a monolayer of binding protein (11, 18, 19). We hypothesized that forming extended chains of the antigen-binding protein would enable the bead to encounter more copies of the tumor antigen, thus reducing the expression level required for cell recovery. Also, because any weak link impairs recovery (11), it is essential that the binding proteins are linked together through irreversible covalent bonds. Therefore, we explored the creation of SpyLigase-assembled protein polymers to enable capture of low-expressing cancer cells.

Results

Design of SpyLigase. SpyTag (13 aa) was left unchanged (15) but the β-strand of CnaB2 containing the reactive Lys was separately expressed and termed KTag (10 aa; Fig. 1*B*). SpyLigase (11 kDa) was derived from SpyCatcher by (*i*) removing residues from the β-strand containing the reactive Lys and (*ii*) circular permutation, replacing residues from the C terminus of CnaB2 with a Gly/Ser linker followed by N-terminal CnaB2 residues (Fig. 1*B*; amino acid sequence in Fig. S1). We hypothesized that SpyTag

Significance

Building proteins into assemblies faces challenges in specificity and stability of the connections. Proteins are ideally connected via peptide tags for minimal disruption of function. *Streptococcus pyogenes* contains a protein that locks itself together. After genetic dissection, we created a protein (SpyLigase) that locks two peptide tags together. With tags on opposite ends of an antibody or affibody (an antibody-like scaffold), SpyLigase assembled the proteins into polyantibody or polyaffibody chains. Magnetic beads can isolate specific cell types, but the small area of bead-to-cell contact means that abundant cell-specific target is required for cell capture. Polymerization of affibodies enabled capture of cancerous cells expressing less cancer marker and should enhance sensitivity of cell isolation for various research and clinical applications.

Author contributions: J.O.F., G.V., and M.H. designed research; J.O.F. and G.V. performed research; J.O.F., G.V., and M.H. analyzed data; and J.O.F., G.V., and M.H. wrote the paper.

Conflict of interest statement: M.H. is an author on a patent application regarding SpyCatcher technology (United Kingdom patent application no. 1002362.0).

This article is a PNAS Direct Submission.

[1]J.O.F. and G.V. contributed equally to this work.

[2]To whom correspondence should be addressed. E-mail: mark.howarth@bioch.ox.ac.uk.

This article contains supporting information online at www.pnas.org/lookup/suppl/doi:10.1073/pnas.1315776111/-/DCSupplemental.

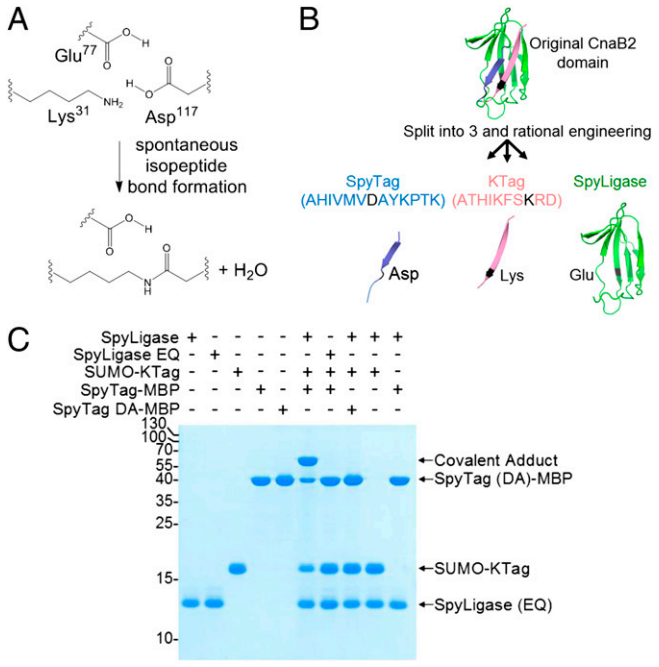

Fig. 1. Principle of SpyLigase design. (*A*) Reaction in CnaB2 domain between Lys and Asp with catalytic Glu to generate an isopeptide bond. (*B*) Splitting of the CnaB2 domain to give three modules. Cartoon of SpyTag peptide (blue), KTag peptide (pink), and SpyLigase (green) from CnaB2 domain (Protein Data Bank ID code 2X5P), with the residues involved in reaction colored black. (*C*) SpyLigase ligated SpyTag to KTag. SpyLigase was mixed with SpyTag-MBP and SUMO-KTag for 24 h before boiling and SDS/PAGE with Coomassie staining. SpyLigase EQ and SpyTag DA-MBP are nonreactive controls.

and KTag would dock with SpyLigase and the triad would be optimally arranged as in CnaB2 to direct covalent ligation of SpyTag with KTag.

SpyLigase Enabled Peptide–Peptide Ligation. KTag fused at the C terminus of small ubiquitin modifier from *Saccharomyces cerevisiae* (SUMO; i.e., SUMO-KTag) and SpyLigase were well expressed in *Escherichia coli* and were soluble at >200 μM (SUMO-KTag) or >800 μM (SpyLigase), with no apparent precipitation upon storage for weeks at 4 °C. We incubated SUMO-KTag with SpyTag fused at the N terminus of maltose binding protein (MBP; i.e., SpyTag-MBP) in the presence of SpyLigase: a new product was generated, stable to boiling in SDS, and with a mobility consistent with isopeptide bond formation between SpyTag and KTag (Fig. 1*C*). With only two of the three components present, with mutation of Glu^{77} to Gln in SpyLigase (i.e., SpyLigase EQ), or with mutation of the reactive Asp in SpyTag (i.e., SpyTag DA-MBP), there was no reaction (Fig. 1*C*).

Dependence of Ligation on Conditions. To explore the generality of the SpyLigase reaction, we added SpyTag and KTag to different termini. SpyLigase was able to drive reaction between SpyTag and KTag at the N terminus or C terminus (Fig. 2*A*). SpyLigase also directed KTag ligation to SpyTag inserted in the middle of a protein (i.e., MBP-SpyTag-Zif-SpyTag, containing SpyTag between MBP and the Zif268 zinc fingers; Fig. 2*B*). We examined the dependence of SpyLigase reaction on temperature: 4 °C gave the highest yield, which gradually decreased as the temperature increased to 37 °C (Fig. 2*C*). The temperature dependence was also studied by CD, showing a change in secondary structure for SpyLigase as temperature was increased from 4 °C to 37 °C (Fig. S2*A*). Usually, proteins show a sharp transition at the melting point by CD as the temperature is increased, but the change was gradual for SpyLigase (Fig. S2*B*), consistent with SpyLigase having a dynamic structure (20).

We confirmed the nature of the covalent reaction between SpyTag and KTag by electrospray-ionization MS. The molecular weight of the SUMO-SpyTag:SUMO-KTag adduct matched the sum of the individual masses (SUMO-SpyTag 13,974 Da; SUMO-KTag 13,703 Da) minus the mass of water, consistent with isopeptide bond formation (Fig. 2*D*).

Generation of Protein Polymers by Using SpyLigase. We used SpyLigase to polymerize affibodies to create multivalent chains for sensitive cell capture. Affibodies are a nonimmunoglobulin scaffold, consisting of a three-helix bundle, selected for high-affinity binding through phage display, and easily expressed in *E. coli* (21). The initial affibody we modified bound strongly and specifically to epidermal growth factor receptor (EGFR) (21), a tyrosine kinase expressed on many cancer cells and a target antigen in CTC isolation (22, 23). We inserted KTag at the N terminus of the affibody and SpyTag at the C terminus (i.e., KTag-AffiEGFR-SpyTag) so that covalent ligation between KTag and SpyTag would generate chains (Fig. 3*A*). Locating the tags at opposite ends was designed to inhibit cyclization. Mixing KTag-AffiEGFR-SpyTag with SpyLigase efficiently generated affibody polymers resistant to boiling in SDS (Fig. 3*B*). No polymers formed with the nonreactive SpyLigase EQ (Fig. 3*B*).

To demonstrate the generality of this SpyLigase approach, we tested a second affibody, binding with high affinity to HER2 (an important tyrosine kinase cancer antigen, also known as ErbB2 or Neu) (23, 24). KTag-AffiHER2-SpyTag was similarly polymerized by SpyLigase, forming high molecular weight species extending to more than 20 affibody units (Fig. 3*C*). A Fab antibody fragment against HER2, bearing SpyTag at the N terminus of the heavy chain and KTag at the C terminus of the light chain, was efficiently expressed in mammalian cells. SpyTag-Fab-KTag was also linked by SpyLigase to generate covalently assembled antibody multimers (Fig. S3).

Affibody Polymers Enhanced Magnetic Cell Capture. We applied KTag-AffiEGFR-SpyTag polymers to enhance the recovery of low antigen-expressing cells for magnetic cancer cell isolation (Fig. 4*A*) (11, 19). Because all of the polymers terminate with a SpyTag, the polymers can be covalently anchored with precise orientation on beads coated with SpyCatcher (15). SpyCatcher itself was linked to the 2.8-μm-diameter beads via a disulfide, so boiling with DTT revealed the affibody polymers attached to the beads (Fig. S4). For the monomeric beads, samples were treated identically to the polymeric beads except the inactive SpyLigase EQ control was used instead of SpyLigase; therefore, a single affibody could attach to each SpyCatcher on the bead but there would not be formation of polymers.

To evaluate the effect of polymerization on cell capture, we studied a panel of cancer cell lines bearing a range of EGFR expression levels: MDA-MB-468 cells express high levels, BT474 cells express low levels, and 771.221 cells do not express detectable levels, as confirmed by flow cytometry (Fig. 4*A*). Monomeric and polymeric beads were incubated with each cell type for 20 min. After magnetic isolation, the efficiency of cell recovery was determined by Coulter counting. Capture by monomeric beads was efficient for the highest expressing cells but recovery was significantly improved with polymeric beads ($n = 3$; $P = 0.03$, unpaired t test; Fig. 4*B*). Beads coated with monomeric affibody could not capture the low-expressing BT474 cells: monomeric beads did not give capture significantly above the background recovery of the nonexpressing 721.221 cells ($n = 3$; $P = 0.09$, not significant, unpaired t test; Fig. 4*C*). However, recovery of BT474 was greatly improved by using polymeric beads ($n = 3$; $P < 0.0001$, unpaired t test; Fig. 4*C*). The use of

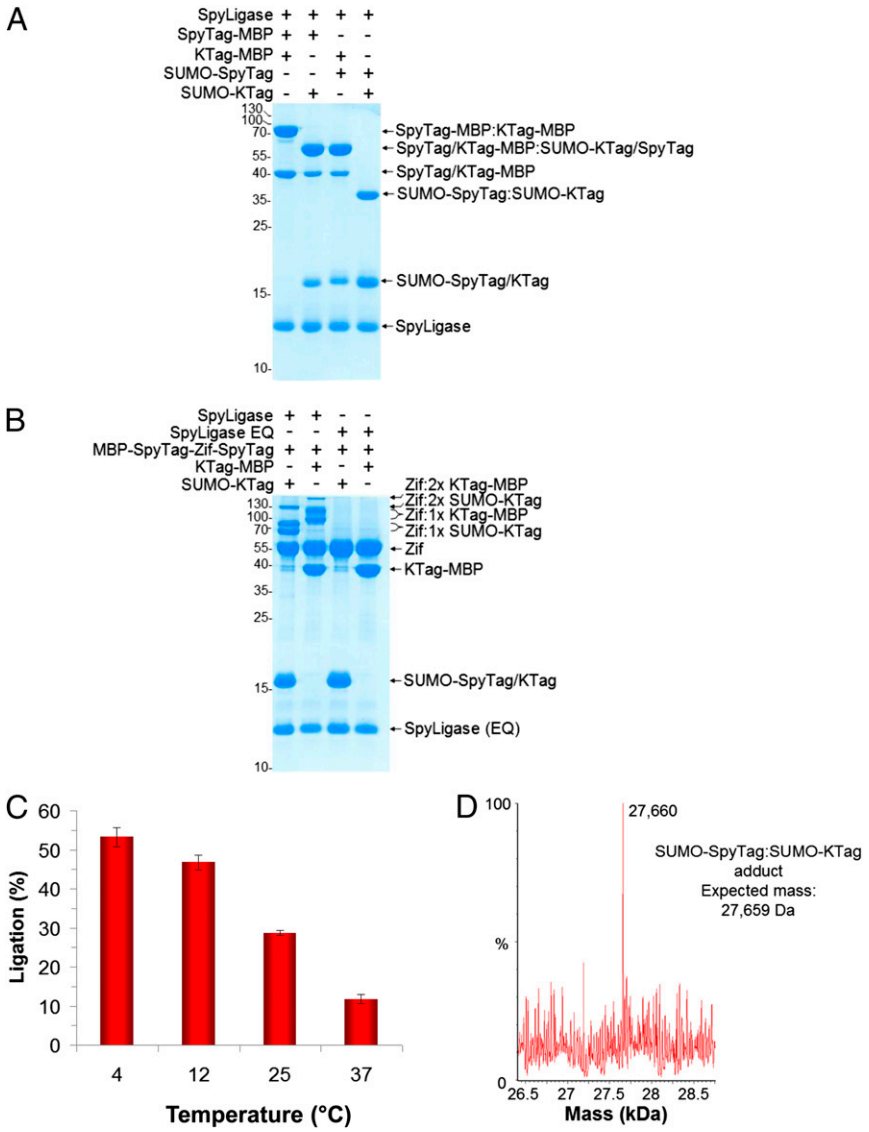

Fig. 2. SpyLigase ligation characteristics. (*A*) SpyLigase ligated SpyTag and KTag at N- and C-termini. Tags were fused N-terminally on MBP or C-terminally on SUMO, incubated with SpyLigase for 24 h, and analyzed by SDS/PAGE with Coomassie staining. (*B*) SpyLigase ligated KTag to internal SpyTag sites, surrounding Zif268, analyzed after 24 h by SDS/PAGE with Coomassie staining. (*C*) Temperature dependence of ligation: SpyLigase was incubated with SpyTag-MBP and SUMO-KTag for 24 h at the indicated temperatures and ligation quantified from SDS/PAGE with Coomassie staining (mean of triplicate ±1 SD). (*D*) Electrospray MS shows SUMO-SpyTag linked to SUMO-KTag after incubation with SpyLigase, with loss of water.

polymeric beads did not change specificity, as background recovery of 721.221 cells was equivalent for monomeric and polymeric beads ($n = 3$; $P = 0.97$, not significant, unpaired t test; Fig. 4*C*).

We previously showed that cell capture sensitivity was greatly improved by acute loading of cells with cholesterol, an important modulator of membrane dynamics and flexibility (11). Cholesterol loading enhanced the recovery of BT474 by using polymeric beads ($n = 3$; $P = 0.01$, unpaired t test) but did not improve recovery with monomeric beads (Fig. S5).

As a further test of affibody polymer efficacy, we generated polymers of an affibody against HER2 by using SpyLigase; when testing recovery of cells doped into a blood sample, polymeric beads gave a highly significant increase in recovery of the high HER2-expressing BT474 ($n = 3$; $P = 0.0005$, unpaired t test) as well as the low HER2-expressing MCF-7 cells ($n = 3$; $P = 0.0001$, unpaired t test; Fig. S6) (11). Polymeric beads did not reduce specificity, as tested by counting recovery of the HER2-negative 721.221 cells, or by fluorescence microscopy showing that recovered cells were carboxyfluorescein succinimidyl ester-positive and negative for CD45, a surface protein common to leukocytes (Fig. S6).

Discussion

There are many examples of proteins split into two that have restored function when the parts reconstitute, including split fluorescent proteins, proteases, and luciferase (25). There are much fewer precedents for splitting a protein into three (26–28). Here we have generated a three-part protein, with a protein domain bringing together and driving reaction between two distinct peptide tags. We have demonstrated here this ligation for SpyTag in six different protein contexts. SpyLigase represents a principle for peptide–peptide ligation not yet found in nature.

Various elegant approaches have been devised to target fluorophores or other small molecules covalently to either peptides (e.g., with FlAsH or Sfp phosphopantetheinyl transferase) or to

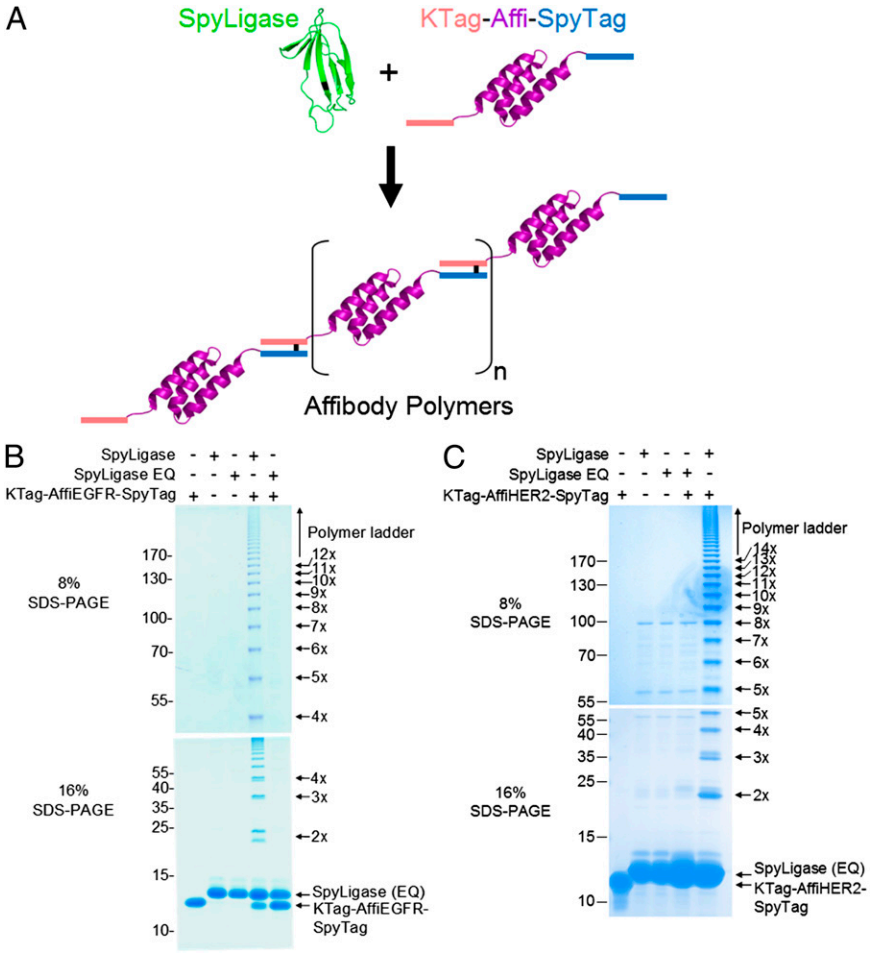

Fig. 3. Affibody polymerization with SpyLigase. (*A*) Cartoon of SpyLigase covalently joining KTag on one affibody to SpyTag on another, so directing polymerization. (*B*) Polymerization of anti-EGFR affibody for 24 h by SpyLigase, analyzed by SDS/PAGE with Coomassie staining. (*C*) Polymerization of anti-HER2 affibody for 48 h by SpyLigase, analyzed by SDS/PAGE with Coomassie staining.

≥20 kDa proteins (e.g., HaloTag and SNAP-tag) (29), but there are few ways to achieve covalent reaction between two genetically encoded peptides. Natural enzymes have been harnessed for peptide ligation, such as transglutaminase, but this enzyme tends to react promiscuously (30). Cys-bearing peptides can associate noncovalently and then form a disulfide, e.g., "dock-and-lock" (31), but adding a new Cys can interfere with folding of existing disulfides. Subtiligase can direct amide bond formation but substrates require an ester-activated C terminus, and its great advantage for proteomics is that almost any N-terminal sequence is reactive (32, 33). Native chemical ligation also allows reaction by using a strategically placed cysteine residue, but, like split inteins and sortase, is limited to the N- and C-termini for fusion of the proteins (34–36), disallowing nonlinear protein architectures. Therefore, SpyLigase, with no cysteine-bearing components and the ability to direct isopeptide bond formation to an internal peptide tag, possesses unique characteristics for protein modification and assembly, although it will be valuable in the future to evolve SpyLigase and its peptide partners for greater speed and yield.

A range of innovative approaches have been taken to enhance CTC capture, including microvortex-generating herringbone chips (37) and microfluidic devices enabling capture of lower expressing cells (38), although magnetic separation has advantages over microfluidics in terms of simplicity and throughput (18, 19). Poly(amidoamine) dendrimers and silicon nanowires have previously given a nanostructured surface enhancing cancer cell capture (39, 40). Polymeric "tentacles" of DNA aptamers also showed promise for rare cell isolation (41). Here we have shown the functional advantage of covalent protein polymerization for capture of cells. Multivalency is a powerful way to enhance biological function and with the right ligand organization gives dramatic improvements in affinity, kinetics and specificity (42, 43). The multivalency of the SpyLigase-assembled affibody polymers enhanced the capture of cancerous cells expressing low levels of tumor antigen, without loss of specificity. Moving protein binders from 2D into 3D via isopeptide-linked protein chains extending from surfaces has potential to enhance detection in a wide variety of areas, including immunoassays, microfluidic cell isolation, and detection of pathogens by nanoparticles (44).

Materials and Methods

In Vitro Reconstitution. *SI Materials and Methods* provides a full description of cloning, protein expression and purification, MS, CD, culture of cell lines, coupling of SpyCatcher to beads, beading from human blood, flow cytometry, and statistical analysis. Briefly, all proteins were expressed in *E. coli*, except for Fab produced in HEK 293T cells, and were purified via Ni-NTA resin.

To test SpyLigase reaction, 10 μM SpyTag-MBP or SpyTag DA-MBP and 10 μM SUMO-KTag were incubated for 24 h at 4 °C with 40 μM SpyLigase or SpyLigase EQ in PCT buffer: 40 mM Na_2HPO_4 and 20 mM citric acid buffer, pH 5.0, with addition of 1.5 M trimethylamine *N*-oxide (TMAO; Sigma-Aldrich) to give final pH 7.0. TMAO is a chemical chaperone (45). To test the

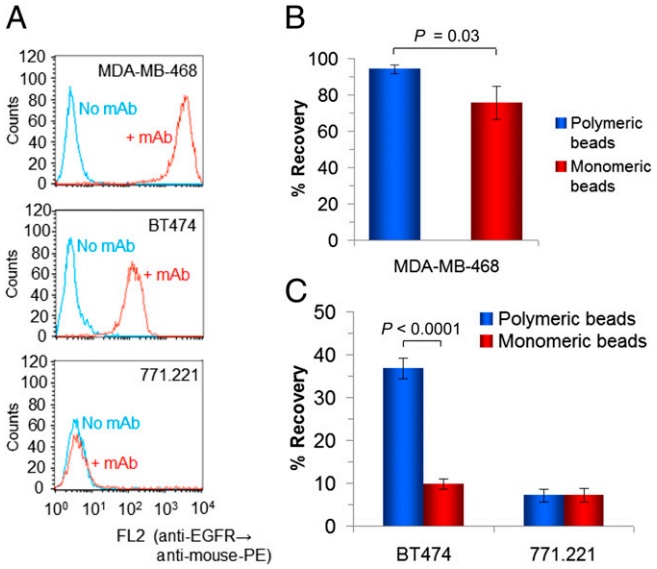

Fig. 4. Enhanced cell capture with affibody polymers. (*A*) Flow cytometry of EGFR expression in three cancer cell lines with the use of anti-EGFR antibody (+mAb, red) or no primary antibody control (no mAb, blue). (*B*) Recovery of high-EGFR MDA-MB-468 using magnetic beads coated with KTag-AffiEGFR-SpyTag affibody polymer (polymeric beads, blue) or affibody monomer (monomeric beads, red; mean of triplicate ±1 SD). (*C*) Recovery of low-EGFR BT474 or nonexpressing 721.221 cells as in *B*.

dependence on N- or C-terminal tag location, 10 μM SUMO-KTag or KTag-MBP was incubated with 10 μM SUMO-SpyTag or SpyTag-MBP under the aforementioned conditions. To test reaction with internal SpyTag, 10 μM MBP-SpyTag-Zif-SpyTag was incubated with 20 μM KTag-MBP or SUMO-KTag under the aforementioned conditions. To test temperature dependence, SUMO-KTag and SpyTag-MBP were incubated with SpyLigase in the same way except at 4, 12, 25, or 37 °C. Reactions were stopped with SDS-loading buffer [0.23 M Tris·HCl, pH 6.8, 24% (vol/vol) glycerol, 120 μM bromophenol blue, 0.23 M SDS] and heated for 5 min at 95 °C in a C1000 Thermal Cycler (Bio-Rad). The samples were then run on SDS/PAGE by using 16% (wt/vol) polyacrylamide gels in an XCell SureLock (Life Technologies) for 75 min at 200 V. Gels were stained with InstantBlue Coomassie stain (Triple Red), imaged with a ChemiDoc XRS+ Imager (Bio-Rad), and quantified by Image Lab Software 3.0 (Bio-Rad). The percentage of ligation was determined as 100× the band intensity of the covalent adduct, divided by the sum of band intensities of the SpyTag-fusion and the KTag-fusion and the covalent adduct.

Affibody and Antibody Polymerization. A total of 100 μM SpyLigase (EQ) was incubated with 38 μM KTag-AffiEGFR-SpyTag for 24 h at 4 °C in 40 mM Na_2HPO_4, 20 mM citric acid, 1 M TMAO, pH 6.8. A small amount of a second band corresponding to twice the molecular weight of KTag-AffiEGFR-SpyTag was seen (Fig. 3*B*), which is most likely from double reaction of $(KTag\text{-}AffiEGFR\text{-}SpyTag)_2$. A total of 76 μM KTag-AffiHER2-SpyTag was incubated with 200 μM SpyLigase (EQ) for 48 h at 4 °C in PCT buffer. A total of 150 μM SpyLigase (EQ) was incubated with 50 μM SpyTag-Fab-KTag for 24 h at 4 °C in PCT buffer.

Coupling of Affibodies for Polymerization on Beads. SpyCatcher beads were washed thrice with PBS solution, then 8.3 μM KTag-AffiEGFR-SpyTag or KTag-AffiHER2b-SpyTag was added to beads and incubated for 2 h at 25 °C with 1,200 rpm shaking on a ThermoMixer comfort (Eppendorf). After incubation, beads were placed on the magnet and uncoupled affibody removed. Beads were split into two vials and washed three times with PBS solution. For polymerization, beads were resuspended in PCT buffer and affibody was added to 76 μM. To polymerize affibody on beads, SpyLigase at a final concentration of 200 μM was added (polymeric beads); for monomeric beads, 200 μM SpyLigase EQ was added. Beads were incubated on a ThermoMixer for 72 h at 4 °C with 1,200 rpm shaking. Polymerization was assessed by SDS/PAGE after boiling in SDS-loading buffer containing 100 mM DTT.

Immunomagnetic Isolation. Immunomagnetic isolation of cells with polymeric and monomeric beads was carried out as previously described (11). Briefly, MDA-MB-468, BT474, and 721.221 cells were harvested and resuspended at 2.5×10^6 cells per milliliter in DMEM with 1% FCS, 50 U/mL penicillin, and 50 μg/mL streptomycin (D1). A total of 100 μL of cells were used per condition. Cells were incubated for 1 h at 25 °C in D1 with 250 μg/mL water-soluble cholesterol (Sigma-Aldrich; rendered water-soluble through the presence of methyl-β-cyclodextrin; cholesterol was withheld in Fig. S5). Then, 12.5 μL monomeric or polymeric beads (based on 2.8-μm diameter DynaBeads), previously washed three times with PBS solution and once with D1, were added to cells, and the volume was adjusted to 500 μL with D1. Cell/bead mixtures were incubated at 25 °C for 20 min with end-over-end rotation. A total of 100 μL of the cell/bead mixture was then pipetted out for counting. The remaining cells were placed onto a magnet. Cells bound to magnetic beads were washed with 500 μL D1 and placed on a ThermoMixer for 30 s at 25 °C with 1,100 rpm shaking. Cells bound to beads were then resuspended in 100 μL D1. Cells were counted on a Coulter Counter (CasyR Model TT; Innovatis) using a 150-μm measuring capillary, with 400 μL sample volume and evaluation cursor of 7.5–50 μm. Percent recovery was calculated as 100 × (number of recovered cells / number of cells originally present).

ACKNOWLEDGMENTS. We thank Michael Fairhead, Jenny Hayes, Bijan Zakeri, and Jayati Jain for assistance in cloning certain constructs; Ryan Baron for phlebotomy; and the University of Oxford Department of Biochemistry Biophysical Facility and Wellcome Trust-funded "Micron" Microscopy Facility. This work was supported by the Medical Research Council (G.V.), the Clarendon Fund (J.O.F.), New College Oxford (J.O.F.), and Merton College Oxford (G.V.).

1. Jarvik JW, Telmer CA (1998) Epitope tagging. *Annu Rev Genet* 32:601–618.
2. Huh WK, et al. (2003) Global analysis of protein localization in budding yeast. *Nature* 425(6959):686–691.
3. Guignet EG, Segura JM, Hovius R, Vogel H (2007) Repetitive reversible labeling of proteins at polyhistidine sequences for single-molecule imaging in live cells. *ChemPhysChem* 8(8):1221–1227.
4. Huang J, Makabe K, Biancalana M, Koide A, Koide S (2009) Structural basis for exquisite specificity of affinity clamps, synthetic binding proteins generated through directed domain-interface evolution. *J Mol Biol* 392(5):1221–1231.
5. Stanfield RL, Wilson IA (1995) Protein-peptide interactions. *Curr Opin Struct Biol* 5(1):103–113.
6. Zakeri B, Howarth M (2010) Spontaneous intermolecular amide bond formation between side chains for irreversible peptide targeting. *J Am Chem Soc* 132(13):4526–4527.
7. Horne WS, Gellman SH (2008) Foldamers with heterogeneous backbones. *Acc Chem Res* 41(10):1399–1408.
8. Fletcher JM, et al. (2013) Self-assembling cages from coiled-coil peptide modules. *Science* 340(6132):595–599.
9. Sainlos M, et al. (2011) Biomimetic divalent ligands for the acute disruption of synaptic AMPAR stabilization. *Nat Chem Biol* 7(2):81–91.
10. Chivers CE, et al. (2010) A streptavidin variant with slower biotin dissociation and increased mechanostability. *Nat Methods* 7(5):391–393.
11. Jain J, Veggiani G, Howarth M (2013) Cholesterol loading and ultrastable protein interactions determine the level of tumor marker required for optimal isolation of cancer cells. *Cancer Res* 73(7):2310–2321.
12. Amelung S, et al. (2011) The FbaB-type fibronectin-binding protein of Streptococcus pyogenes promotes specific invasion into endothelial cells. *Cell Microbiol* 13(8):1200–1211.
13. Hagan RM, et al. (2010) NMR spectroscopic and theoretical analysis of a spontaneously formed Lys-Asp isopeptide bond. *Angew Chem Int Ed Engl* 49(45):8421–8425.
14. Kang HJ, Baker EN (2011) Intramolecular isopeptide bonds: Protein crosslinks built for stress? *Trends Biochem Sci* 36(4):229–237.
15. Zakeri B, et al. (2012) Peptide tag forming a rapid covalent bond to a protein, through engineering a bacterial adhesin. *Proc Natl Acad Sci USA* 109(12):E690–E697.
16. Powles R, et al. (2000) Allogeneic blood and bone-marrow stem-cell transplantation in haematological malignant diseases: A randomised trial. *Lancet* 355(9211):1231–1237.
17. Stift A, et al. (2003) Dendritic cell-based vaccination in solid cancer. *J Clin Oncol* 21(1):135–142.
18. Yu M, Stott S, Toner M, Maheswaran S, Haber DA (2011) Circulating tumor cells: Approaches to isolation and characterization. *J Cell Biol* 192(3):373–382.
19. Dharmasiri U, Witek MA, Adams AA, Soper SA (2010) Microsystems for the capture of low-abundance cells. *Annu Rev Anal Chem (Palo Alto Calif)* 3:409–431.
20. Vamvaca K, Vögeli B, Kast P, Pervushin K, Hilvert D (2004) An enzymatic molten globule: Efficient coupling of folding and catalysis. *Proc Natl Acad Sci USA* 101(35):12860–12864.
21. Friedman M, et al. (2008) Directed evolution to low nanomolar affinity of a tumor-targeting epidermal growth factor receptor-binding affibody molecule. *J Mol Biol* 376(5):1388–1402.
22. Zhang L, et al. (2013) The identification and characterization of breast cancer CTCs competent for brain metastasis. *Sci Transl Med* 5(180):80ra48.
23. Mayer JA, et al. (2011) FISH-based determination of HER2 status in circulating tumor cells isolated with the microfluidic CEE™ platform. *Cancer Genet* 204(11):589–595.

24. Eigenbrot C, Ultsch M, Dubnovitsky A, Abrahmsén L, Härd T (2010) Structural basis for high-affinity HER2 receptor binding by an engineered protein. *Proc Natl Acad Sci USA* 107(34):15039–15044.
25. Ozawa T (2006) Designing split reporter proteins for analytical tools. *Anal Chim Acta* 556(1):58–68.
26. Lin MC, Gutte B, Moore S, Merrifield RB (1970) Regeneration of activity by mixture of ribonuclease enzymically degraded from the COOH terminus and a synthetic COOH-terminal tetradecapeptide. *J Biol Chem* 245(19):5169–5170.
27. Sun W, Yang J, Liu XQ (2004) Synthetic two-piece and three-piece split inteins for protein trans-splicing. *J Biol Chem* 279(34):35281–35286.
28. Kellermann SJ, Rath AK, Rentmeister A (2013) Tetramolecular fluorescence complementation for detection of specific RNAs in vitro. *ChemBioChem* 14(2):200–204.
29. Marks KM, Nolan GP (2006) Chemical labeling strategies for cell biology. *Nat Methods* 3(8):591–596.
30. Hitomi K, Kitamura M, Sugimura Y (2009) Preferred substrate sequences for transglutaminase 2: Screening using a phage-displayed peptide library. *Amino Acids* 36(4): 619–624.
31. Rossi EA, Goldenberg DM, Chang CH (2012) Complex and defined biostructures with the dock-and-lock method. *Trends Pharmacol Sci* 33(9):474–481.
32. Jackson DY, et al. (1994) A designed peptide ligase for total synthesis of ribonuclease A with unnatural catalytic residues. *Science* 266(5183):243–247.
33. Wildes D, Wells JA (2010) Sampling the N-terminal proteome of human blood. *Proc Natl Acad Sci USA* 107(10):4561–4566.
34. Kent SB (2009) Total chemical synthesis of proteins. *Chem Soc Rev* 38(2):338–351.
35. Shah NH, Muir TW (2011) Split inteins: Nature's protein ligases. *Isr J Chem* 51(8-9): 854–861.
36. Popp MW, Antos JM, Grotenbreg GM, Spooner E, Ploegh HL (2007) Sortagging: A versatile method for protein labeling. *Nat Chem Biol* 3(11):707–708.
37. Stott SL, et al. (2010) Isolation of circulating tumor cells using a microvortex-generating herringbone-chip. *Proc Natl Acad Sci USA* 107(43):18392–18397.
38. Ozkumur E, et al. (2013) Inertial focusing for tumor antigen-dependent and -independent sorting of rare circulating tumor cells. *Sci Transl Med* 5(179):79ra47.
39. Myung JH, Gajjar KA, Saric J, Eddington DT, Hong S (2011) Dendrimer-mediated multivalent binding for the enhanced capture of tumor cells. *Angew Chem Int Ed Engl* 50(49):11769–11772.
40. Wang S, et al. (2011) Highly efficient capture of circulating tumor cells by using nanostructured silicon substrates with integrated chaotic micromixers. *Angew Chem Int Ed Engl* 50(13):3084–3088.
41. Zhao W, et al. (2012) Bioinspired multivalent DNA network for capture and release of cells. *Proc Natl Acad Sci USA* 109(48):19626–19631.
42. Carlson CB, Mowery P, Owen RM, Dykhuizen EC, Kiessling LL (2007) Selective tumor cell targeting using low-affinity, multivalent interactions. *ACS Chem Biol* 2(2):119–127.
43. Albertazzi L, et al. (2013) Spatiotemporal control and superselectivity in supramolecular polymers using multivalency. *Proc Natl Acad Sci USA* 110(30):12203–12208.
44. Shao H, et al. (2012) Magnetic nanoparticles and microNMR for diagnostic applications. *Theranostics* 2(1):55–65.
45. Yancey PH (2004) Compatible and counteracting solutes: Protecting cells from the Dead Sea to the deep sea. *Sci Prog* 87(pt 1):1–24.

Supporting Information

Fierer et al. 10.1073/pnas.1315776111

SI Materials and Methods

Cloning. All amplifications were done with KOD Hot Start DNA Polymerase (Roche). Numbering of residues in SpyLigase is based on the sequence of CnaB2 from Protein Data Bank ID code 2X5P (1), a domain from FbaB of *Streptococcus pyogenes* strain MGAS315, expressed in pDEST14 (2). pDEST14-SpyLigase (GenBank KJ401122, Addgene ID 51722) was produced in three steps from pDEST14-SpyCatcher (3). The initial deletion removed the KTag β-strand by PCR using 5′-GAGCAAGGTCAGTCCGGTGACGGCAAAGAGTTAGC and 5′-GCTAACTCTTTGCCGTCACCGGACTGACCTTGCTC. This construct was truncated via site-directed, ligase-independent mutagenesis (SLIM) PCR (4) using 5′-GTCGTACTACCATCACCATCACCATCACGATTACGACGGTCAGTCCGGTGACGGC, 5′-GTCGTAATCGTGATGGTGATGGTGATGGTAGTACGAC, 5′-CACCATCACGATTACGACGGTCAGTCCGGTGACGGCAAAGAGTTAGCTG, and 5′-CAGCTAACTCTTTGCCGTCACCGGACTGACC. The construct was then modified by the addition of a GS linker at the C terminus followed by a circular permutation (Fig. S1) via SLIM PCR using 5′-GCAAGGTCAGGTTACTGTAAATGGCAAAGCAACTAAAGGTGGGAGTGGTGGCAGCGGAGGTAGTGGCGAGGACAGCGCTACCCATATT, 5′-ACCTTTAGTTGCTTTGCCATTTACAGTAACCTGACCTTGC, 5′-GGGAGTGGTGGCAGCGGAGGTAGTGGCGAGGACAGCGCTACCCATATTTAAATGGTTGATGCTTGAGGATCCGAATTCGAGC, and 5′-GCTCGAATTCGGATCCTCAAGCATCAACCATTTA. pDEST14-SpyLigase EQ was generated by QuikChange from pDEST14-SpyLigase using 5′-GGAAAATATACATTTGTCCAAACCGCAGCACCAGACG and 5′-CGTCTGGTGCTGCGGTTTGGACAAATGTATATTTTCC.

SpyTag linked to the N terminus of maltose binding protein (MBP; pET28a-SpyTag-MBP), SpyTag-MBP with the reactive Asp changed to Ala (pET28a-SpyTag DA-MBP), and MBP followed by the Zif268 zinc fingers with SpyTag on each side (pET28a-MBP-SpyTag-Zif-SpyTag) were previously described (3). pET28a-SUMO-KTag (Addgene ID 51723) was cloned by PCR of small ubiquitin modifier from *Saccharomyces cerevisiae* (SUMO) from pOPINS (5) (gift from Ray Owens, University of Oxford, Oxford, United Kingdom) with 5′-TATACCATGGGTAGCAGCCATC and 5′-GTGAAGCTTAATAACCATCACGTTTTGAGAATTTAATATGGGTAGCGCCACCACCGATCTGTTCGCG, digested with NcoI and HindIII, and then ligated into similarly digested pET28a. pET28a-SUMO-SpyTag was generated from pET28a-SUMO-KTag using SLIM with 5′-GCATCGCGAACAGATCGGTGGTGGCGCCCACATCGTGATGGTGGACGCCTACAAGCCGACGAAG, 5′-GCCACCACCGATCTGTTCGCGATGC, 5′-CTCGAGTGCGGCCGCAAGCTTAATAACC, and 5′-CCCACATCGTGATGGTGGACGCCTACAAGCCGACGAAGGGTTATTAAGCTTGCGGCCGCACTCGAG. pDEST14-Cys-SpyCatcher, containing Cys following the His_6-tag, was generated by QuikChange from pDEST14-SpyCatcher using 5′-CACCATCACCATCACGATTGCGACATCCCAACGACCGAAAACC and 5′-GGTTTTCGGTCGTTGGGATGTCGCAATCGTGATGGTGATGGTG.

pET28a-KTag-AffiEGFR-SpyTag was generated by PCR from pET21b-Affibody $Z_{EGFR:1907}$ (6, 7) using 5′-AGGACCATGGGCGCTACCCATATTAAATTCTCAAAACGTGATGGTTCTGGAGCTAGCATGACTGGTGGACAGCAAATGG and 5′-TTTAAAGCTTTTATCACTTCGTCGGCTTGTAGGCGTCCACCATCACGATGTGGGCGCCGGATCCGTGGTGGTGGTGGTGGTGCTCGAG, digestion with NcoI and HindIII, and ligation into complementary sites on pET28a.

pET28a-KTag-AffiHER2-SpyTag, based on $Z_{HER2:342}$ (8), was cloned by inverse PCR using pET28a-KTag-AffiEGFR-SpyTag as a template, digesting with DpnI and ligating using T4 DNA ligase before transformation.

pET28a-KTag-AffiHER2b-SpyTag, bearing N23T S33K mutations in the affibody framework to reduce immunoglobulin binding (9), was cloned by inverse PCR using pET28a-KTag-AffiEGFR-SpyTag as a template with 5′-GGGTAAAAGAGCTATCTCCCAGTAAGCGTTCCTCATTTCTTTGTTGAATTTGTTGTCCACGCCCGG and 5′-AACTTAACCAATCAACAGAAAAGGGCTTTCATAAGGAAATTATACGATGACCCAAGCCAAAGCGCTAAC.

pET28a-KTag-MBP was cloned by PCR of MBP from pMAL (New England Biolabs) using 5′-GGGGCATATGGGAGCTACCCATATTAAATTCTCAAAACGTGATGGTAGTGGTGAAAGTGGTAAAATCGAAGAAGGTAAA and 5′-GGGGAAGCTTTTACGAGCTCGAATTAGTCTG, digested with NdeI and HindIII, and ligated into digested pET28a.

SpyTag-Fab-KTag was assembled from the SpyTag-4D5 heavy chain and the hu4D5-KTag light chain. The murine variable heavy chain (4D5 Vh) (10) was synthesized using DNAWorks (11) and inserted into pOPINVh (gift from Ray Owens, University of Oxford, Oxford, United Kingdom) (12) via KpnI and SfoI digestion. SpyTag was added at the N terminus, using pOPINVh 4D5 as template, via SLIM PCR. Going from the N terminus, the heavy chain construct contained a signal sequence (cleaved in the endoplasmic reticulum), SpyTag, GSG linker, matrix metalloproteinase-9 cleavage site (VVPLSLR), Vh domain, CH1 domain, and a His_6 tag.

hu4D5-KTag light chain was produced in two steps from Fab0.11 (13). Insertion of KTag at the C terminus of the light chain was achieved by PCR and ligation into pOPINVl (gift from Ray Owens, University of Oxford, Oxford, United Kingdom) (12), using KpnI and PmeI digestion. This construct was used as template for PCR to add GY at the C terminus using 5′-GCTACCCATATTAAATTCTCAAAACGTGATGGTTATTAATAAGTTTAAACGATCAAAACGATCAAACATCACCATCAC and 5′-GTGATGGTGATGTTTGATCGTTTTGATCGTTTAAACTTATTAATAACCATCACGTTTTGAGAATTTAATATGGGTAGC. PCR products were digested with KpnI and PmeI, and then ligated into similarly digested pOPINVl. The light chain construct had a signal sequence (cleaved in the endoplasmic reticulum), Vl domain, Cκ domain, KTag, and C-terminal GY dipeptide. All constructs and mutations were verified by sequencing.

Protein Expression and Purification from Bacteria. pDEST14 constructs were expressed in *Escherichia coli* BL21 DE3 pLysS (Stratagene), whereas pET28a constructs were expressed in *E. coli* BL21 DE3 RIPL (Agilent). Overnight cultures at 37 °C in Luria-Bertani broth and 0.8% glucose were grown with kanamycin (0.5 mg/mL) for pET28a vectors and ampicillin (0.1 mg/mL) for pDEST14 vectors. The overnight cultures were then diluted 1:100, grown to an OD_{600} of 0.5–0.6, and induced with 0.4 mM IPTG at 30 °C for 4 h. Proteins were purified by using standard methods on Ni-NTA, except for MBP-SpyTag-Zif-SpyTag, which was purified on amylose–agarose as described previously (3). After elution, all proteins were dialyzed three times in a 1,000-fold excess of PBS solution for at least 3 h each time at 4 °C. Protein concentration was determined by using the Micro Bicinchoninic Acid Assay kit (Thermo Scientific), following the manufacturer's instructions. Typical yields per liter of

culture were 7 mg for SUMO fusions, 16 mg for MBP fusions, and 20 mg for SpyLigase.

Protein Expression and Purification from Mammalian Cells. SpyTag-Fab-KTag was expressed in HEK 293T cells grown in roller bottles (Greiner) in 250 mL DMEM with 10% (vol/vol) FCS, 50 U/mL penicillin, and 50 μg/mL streptomycin. HEK 293T cells were transfected in serum-free DMEM with 50 U/mL penicillin and 50 μg/mL streptomycin, using 1.15 mg polyethyleneimine (25 kDa; Sigma) with 160 μg heavy-chain plasmid and 160 μg light-chain plasmid. These plasmids were endotoxin-free, prepared using the Fisher Maxiprep kit. A total of 25 mM Hepes, 3.8 mM valproic acid (Sigma), and 4 mM glutamine (Life Technologies) were added at transfection. Four days following transfection, the supernatant was harvested using centrifugation at 4,000 × *g* for 20 min at 4 °C. A total of 25 mL 10× PBS and $MgCl_2$ to a final concentration of 100 μM were added to the supernatant. Fab was purified by using standard methods on Ni-NTA, as described previously (13), and dialyzed three times in a 1,000-fold excess of PBS solution for at least 3 h each time at 4 °C. Protein concentration was determined from OD_{280} with the extinction coefficient from ExPASy ProtParam. Typical yield was 6 mg per liter of culture.

MS. A total of 10 μM SUMO-KTag, 10 μM SUMO-SpyTag, and 40 μM SpyLigase were incubated for 24 h in 40 mM Na_2HPO_4 and 20 mM citric acid buffer, pH 5.0, with addition of 1.5 M trimethylamine *N*-oxide (Sigma-Aldrich) to give final pH 7.0 (PCT buffer) at 4 °C. The samples were spin-filtered to enrich the SUMO-KTag:SUMO-SpyTag adduct using a Vivaspin 30,000 molecular weight cutoff column (Sartorius). Before analysis, the protein samples were extracted with a C4 ZipTip (Millipore). MS was performed in positive ion mode in 50% (vol/vol) acetonitrile/water, 0.1% formic acid, using a Micromass LCT time-of-flight electrospray ionization MS (Micromass). MassLynx V4.00.00 software (Waters) converted the *m/z* spectrum to molecular mass by using a maximum entropy algorithm. ExPASy ProtParam predicted mass based on the sequence, with the N-terminal fMet residues cleaved.

CD. Far-UV CD spectra of SpyLigase were recorded by using a Jasco J-815 spectropolarimeter. Samples were analyzed in 0.5-mm path-length quartz cuvettes at 0.5 mg/mL in PCT buffer. Far-UV spectra were recorded between 205 and 260 nm at 4, 12, 25, and 37 °C and data were collected at 0.2-nm intervals. Three scans were recorded, averaged for each spectrum, and smoothed with a Savitzky–Golay filter (14) by using Jasco J-815 Spectra Manager software. The temperature-dependent profile of SpyLigase was recorded between 215 and 250 nm, ramping from 4 °C to 90 °C at 2 °C/min.

Culture of Cell Lines. MDA-MB-468 cells (human breast cancer cell line) were from American Type Culture Collection, and BT474 and MCF-7 (human breast cancer cell-lines) were from Cancer Research UK at Lincoln's Inn Fields, and LBL 721.221 cells (human lymphoblastoid cell line) were a gift from Tim Elliott (University of Southampton, Southampton, United Kingdom). Cells were grown in DMEM with 10% (vol/vol) FCS, 50 U/mL penicillin, and 50 μg/mL streptomycin. Insulin (Sigma-Aldrich) was added to BT474 cells at 5 μg/mL. All cells were passaged for fewer than 6 mo. For *Mycoplasma* testing, 1 mL cell culture supernatant from each cell line in a 1.5-mL microcentrifuge tube was spun for 3 min at 1,700 × *g* to pellet cellular debris. The obtained supernatant was transferred to a new tube and spun for 10 min at 17,000 × *g* to sediment *Mycoplasma*. The supernatant was decanted and the pellet (not visible) was resuspended with 50 μL MilliQ water and mixed thoroughly. Samples were heated for 3 min at 95 °C and then *Mycoplasma* presence was assessed by PCR by using 5′-GGGAGCAAACAGGATTAGATACCCT and 5′-TGCACCATCTGTCACTCTGTTAACCTC with Taq DNA Polymerase (NEB). Samples were heated at 94 °C for 0.5 min and then processed for 35 cycles heating at 94 °C for 2 min, 60 °C for 2 min, and 72 °C for 1 min. Samples were finally heated for one cycle at 94 °C for 0.5 min, 60 °C for 2 min, and 72 °C for 5 min. The positive control was the PCR template from the EZ-PCR *Mycoplasma* test (Biological Industries). Amplified products were detected by loading onto an ethidium bromide-stained 2% (wt/vol) agarose gel, imaged under UV by a ChemiDoc XRS+ Imager. The cell lines tested negative for *Mycoplasma*.

Coupling of Cys-SpyCatcher to Beads. Dynabeads M-270 Amine (2.8-μm diameter superparamagnetic polystyrene beads with primary amino functionalities on their surface, 2×10^9 beads per milliliter; Life Technologies) were washed thrice with PBS solution with 0.1 M $NaHCO_3$, pH 8.0 (coupling buffer). A solution of sulfosuccinimidyl 6-(3′-[2-pyridyldithio]-propionamido)hexanoate (Thermo Scientific) was added to beads at a final concentration of 2.5 mM and incubated on a ThermoMixer for 1 h at 25 °C with 1,000 rpm shaking. Beads were then placed onto a magnet (MagRack 6, GE Healthcare) and excess sulfosuccinimidyl 6-(3′-[2-pyridyldithio]-propionamido)hexanoate removed. After washing beads thrice with PBS solution, beads were resuspended at 2×10^9 beads per milliliter in 200 μM Cys-SpyCatcher, for disulfide-mediated attachment for 16 h at 25 °C with 1,000 rpm shaking. Beads were washed thrice with PBS solution containing 0.5% BSA and 0.1% Triton-X-100, resuspended in PBS solution containing 3% (wt/vol) BSA and 0.05% sodium azide, and incubated for 1 h at 25 °C with 1,000 rpm shaking. Beads were washed thrice more with PBS solution, resuspended in PBS solution containing 0.5% BSA and 0.05% sodium azide, and stored at 4 °C.

Beading from Human Blood. BT474, MCF-7 or 771.221 cells were harvested and washed with PBS solution containing 1% FCS, before resuspension at 10^6 cells per milliliter in PBS solution containing 1% FCS. Carboxyfluorescein succinimidyl ester (CFSE; Sigma-Aldrich) was added at a final concentration of 10 μM and incubated at 37 °C in the dark for 15 min. Labeled cells were spun at 250 × *g* for 3 min, resuspended in DMEM with 10% (vol/vol) FCS, 50 U/mL penicillin, and 50 μg/mL streptomycin, and incubated at 37 °C in the dark for a further 30 min. Cells were spun at 250 × *g* for 3 min and resuspended in DMEM with 1% FCS, 50 U/mL penicillin, and 50 μg/mL streptomycin (D1) containing protease inhibitors. Protease inhibitors, in each case, were a 1:100 dilution from a stock of one Complete mini EDTA-free protease inhibitor tablet (Roche) dissolved in 1.5 mL MilliQ water. A total of 250,000 cells were spiked into 1 mL of human blood obtained from a healthy donor. The protocol, including the use and handling of human blood, was approved by the University of Oxford Central University Research Ethics Committee.

Samples were transferred into red blood cell lysis buffer (154 mM NH_4Cl, 10 mM $KHCO_3$, 0.1 mM EDTA, pH 7.2, containing protease inhibitors) at the ratio of 25 mL lysis buffer per 1 mL blood and incubated at 25 °C for 7 min. Cells were spun at 250 × *g* for 3 min, and the pellet was washed twice with 1 mL D1 containing protease inhibitors. Cells were incubated for 1 h at 25 °C in 100 μL D1 with 250 μg/mL water-soluble cholesterol (Sigma-Aldrich) and protease inhibitors. Immunomagnetic isolation was performed by using KTag-AffiHER2b-SpyTag following the procedure described in *Materials and Methods*. Following isolation, samples were washed with 400 μL PBS solution and then fixed by resuspending cells in 100 μL PBS solution containing 4% (wt/vol) formaldehyde and incubating for 10 min at 25 °C. Cells were washed once with 400 μL PBS solution and labeled with 100 μL per sample of 1:20 goat anti-human CD45-phycoerythrin (PE; Life Technologies) for 10 min

at 25 °C in the dark. Excess antibody was removed by placing samples on a magnet and washing cells with 200 μL PBS solution before resuspending in 30 μL PBS solution. As a positive control for CD45 staining, a human whole-blood sample was incubated with lysis buffer and washed as described earlier, but was fixed and stained without any magnetic isolation.

Microscopy. Cells were imaged in a hemocytometer using a 4× lens on an inverted DeltaVision wide-field fluorescence microscope (Applied Precision). Data in the FITC channel for CFSE (490DF20 excitation, 528DF38 emission, Chroma 84100bs polychroic), TRITC channel for PE (555DF28 excitation, 617DF73 emission, Chroma 84100bs polychroic) and bright-field images were collected and analyzed using softWoRx 3.6.2 software (Applied Precision). Background was corrected with the same software. Typical exposure times were 0.25–2 s. Different samples from the same experiment were prepared, imaged, and analyzed by using identical conditions.

Flow Cytometry. Cells were harvested and resuspended at 2.5×10^6 cells per milliliter. A total of 125,000 cells per sample were incubated in PBS solution containing 1% BSA and 0.1% NaN_3 (FACS-A buffer) with or without 10 μg/mL mouse anti-human EGFR (Ab-1 clone 528; Millipore) for 10 min at 25 °C. Antibody excess was removed by centrifugation. Samples were washed thrice with 100 μL FACS-A buffer. A total of 100 μL per sample of 1:100 goat anti-mouse IgG-PE (Life Technologies) in FACS-A buffer was added to samples, and cells were incubated for 10 min on ice. Cells were spun at $368 \times g$ for 3 min at 4 °C and washed thrice with 100 μL FACS-A buffer. Samples were resuspended in 300 μL FACS-A buffer on ice and analyzed on a FACScalibur flow cytometer with CellQuest Pro version 5.2.1 software (Becton Dickinson).

Statistical Analysis. Statistical tests were unpaired two-tailed *t* tests and were performed with GraphPad software QuickCalcs.

1. Oke M, et al. (2010) The Scottish Structural Proteomics Facility: Targets, methods and outputs. *J Struct Funct Genomics* 11(2):167–180.
2. Hagan RM, et al. (2010) NMR spectroscopic and theoretical analysis of a spontaneously formed Lys-Asp isopeptide bond. *Angew Chem Int Ed Engl* 49(45): 8421–8425.
3. Zakeri B, et al. (2012) Peptide tag forming a rapid covalent bond to a protein, through engineering a bacterial adhesin. *Proc Natl Acad Sci USA* 109(12):E690–E697.
4. Chiu J, March PE, Lee R, Tillett D (2004) Site-directed, ligase-independent mutagenesis (SLIM): A single-tube methodology approaching 100% efficiency in 4 h. *Nucleic Acids Res* 32(21):e174.
5. Berrow NS, et al. (2007) A versatile ligation-independent cloning method suitable for high-throughput expression screening applications. *Nucleic Acids Res* 35(6):e45.
6. Friedman M, et al. (2008) Directed evolution to low nanomolar affinity of a tumor-targeting epidermal growth factor receptor-binding affibody molecule. *J Mol Biol* 376(5):1388–1402.
7. Friedman M, et al. (2007) Phage display selection of Affibody molecules with specific binding to the extracellular domain of the epidermal growth factor receptor. *Protein Eng Des Sel* 20(4):189–199.
8. Orlova A, et al. (2006) Tumor imaging using a picomolar affinity HER2 binding affibody molecule. *Cancer Res* 66(8):4339–4348.
9. Feldwisch J, et al. (2010) Design of an optimized scaffold for affibody molecules. *J Mol Biol* 398(2):232–247.
10. Carter P, et al. (1992) Humanization of an anti-p185HER2 antibody for human cancer therapy. *Proc Natl Acad Sci USA* 89(10):4285–4289.
11. Hoover DM, Lubkowski J (2002) DNAWorks: An automated method for designing oligonucleotides for PCR-based gene synthesis. *Nucleic Acids Res* 30(10):e43.
12. Nettleship JE, et al. (2008) A pipeline for the production of antibody fragments for structural studies using transient expression in HEK 293T cells. *Protein Expr Purif* 62(1): 83–89.
13. Jain J, Veggiani G, Howarth M (2013) Cholesterol loading and ultrastable protein interactions determine the level of tumor marker required for optimal isolation of cancer cells. *Cancer Res* 73(7):2310–2321.
14. Savitzky A, Golay MJE (1964) Smoothing + differentiation of data by simplified least squares procedures. *Anal Chem* 36:1627–1639.

```
CnaB2       MSYYHHHHHHDYDIPTTENLYFQGAMVDTLSGLSSEQGQSGDMTIEEDSATHIKFSKRDI
SpyCatcher  MSYYHHHHHHDYDIPTTENLYFQGAMVDTLSGLSSEQGQSGDMTIEEDSATHIKFSKRDE
SpyLigase   MSYYHHHHHHDYD------------------------GQSG--------------------

CnaB2       DGKELAGATMELRDSSGKTISTWISDGQVKDFYLMPGKYTFVETAAPDGYEVATAITFTV
SpyCatcher  DGKELAGATMELRDSSGKTISTWISDGQVKDFYLYPGKYTFVETAAPDGYEVATAITFTV
SpyLigase   DGKELAGATMELRDSSGKTISTWISDGQVKDFYLYPGKYTFVETAAPDGYEVATAITFTV

CnaB2       NEQGQVTVNGKATKGDAHIVMVDA-------
SpyCatcher  NEQGQVTVNGKATKGDAHI------------
SpyLigase   NEQGQVTVNGKATKGGSGGSGGSGEDSATHI

            SpyTag      AHIVMVDAYKPTK
            KTag        ATHIKFSKRD
```

TEV protease cleavage site
I→E and M→Y mutations in SpyCatcher compared to original CnaB2
SpyTag parent sequence
KTag parent sequence
Circular Permutation

Fig. S1. Sequence alignment of the parent CnaB2 domain, expressed with an N-terminal His6-tag and TEV protease cleavage site, compared with the SpyCatcher domain (reacting itself with SpyTag) and SpyLigase (directing SpyTag to react with KTag).

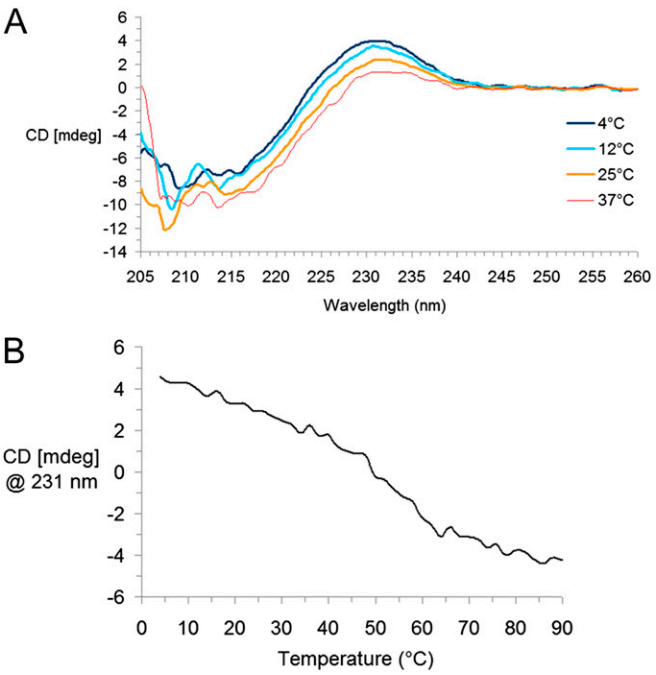

Fig. S2. Analysis of SpyLigase secondary structure by circular dichroism. (*A*) Far-UV CD spectrum of SpyLigase in PCT buffer at 4, 12, 25, or 37 °C. (*B*) SpyLigase CD intensity at 231 nm (the peak from the spectrum above), from 4 °C and increasing to 90 °C, in PCT buffer.

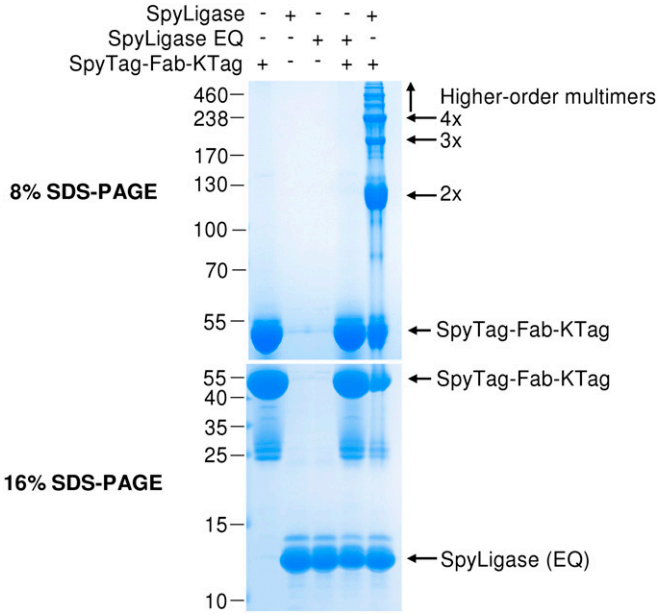

Fig. S3. Antibody polymerization using SpyLigase. SpyTag-Fab-KTag, based on the anti-HER2 Fab 4D5, purified from HEK 293T cells, was incubated for 24 h with SpyLigase or the negative control SpyLigase EQ. Protein samples were boiled in SDS without DTT and analyzed by SDS/PAGE with Coomassie staining. The 8% and 16% polyacrylamide gels are shown.

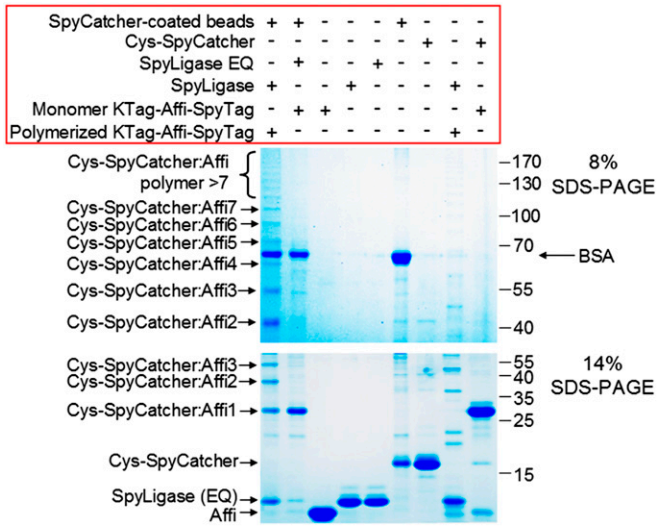

Fig. S4. Analysis of affibody polymers on beads. KTag-AffiEGFR-SpyTag (Affi) polymerized on magnetic beads. Samples were boiled with DTT and analyzed by SDS/PAGE with Coomassie staining. Monomer KTag-AffiEGFR-SpyTag and polymerized KTag-AffiEGFR-SpyTag were also analyzed in the absence of beads. The 66-kDa band corresponding in molecular weight to BSA was present in the initial bead preparation and was not removed by prolonged washing. Bands eluted from the beads are marked corresponding to Cys-SpyCatcher covalently linked to different numbers of affibodies (separated by ~12 kDa).

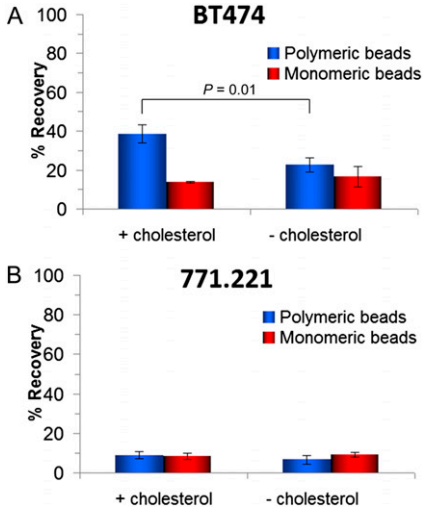

Fig. S5. Effect of cholesterol loading on cell recovery. (*A*) BT474 or (*B*) 721.221 were incubated for 60 min with or without cholesterol, before magnetic cell isolation by using polymeric or monomeric KTag-AffiEGFR-SpyTag beads and Coulter counting (mean of triplicate ±1 SD).

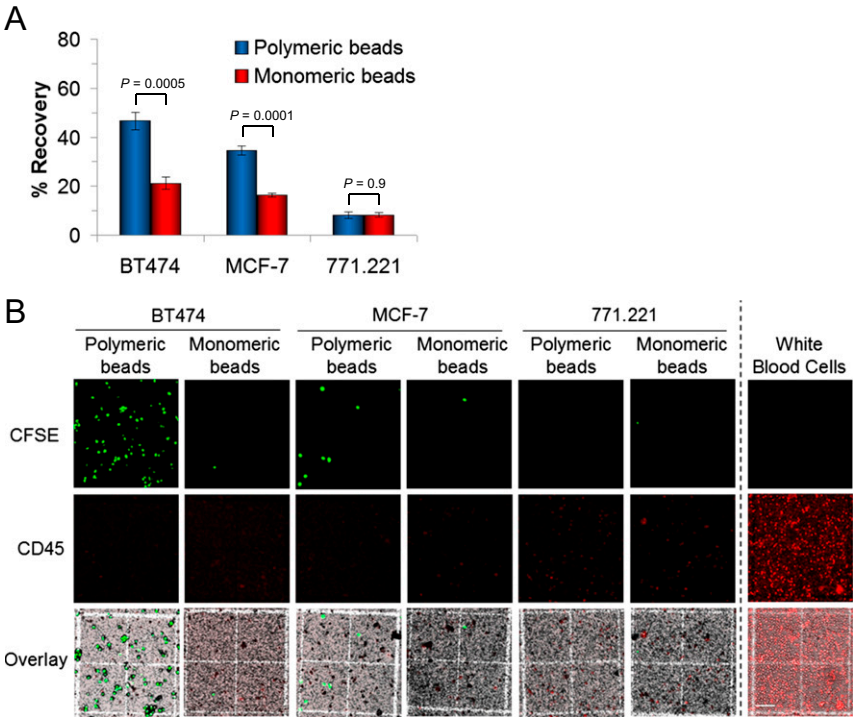

Fig. S6. Effect of affibody polymerization on cell capture from blood. (*A*) Cells with high (BT474), low (MCF-7), or no (721.221) HER2 expression were doped into human blood before incubation with magnetic beads coated with KTag-AffiHER2b-SpyTag monomer or polymer and then Coulter counting of recovered cells (mean of triplicate ±1 SD). (*B*) Fluorescence microscopy of cells recovered from blood, using beads coated with polymeric or monomeric affibody. CFSE (*Top*) marks the cell lines and anti-CD45 (*Middle*) the leukocytes also recovered. (*Bottom*) Overlay of CFSE (green), anti-CD45 (red), and bright-field (grayscale) images. The white blood cell sample (from whole blood, after red blood cell lysis but without magnetic separation) acted as a positive control for CD45 staining.